

# Investigating the effects of pyridine and poly(4-vinylpyridine) on CO<sub>2</sub> reduction electrocatalysis at gold electrodes using *in-situ* surface-enhanced Raman spectroelectrochemistry

James J. Walsh\* <sup>a, b</sup>

<sup>a</sup>: National Centre for Sensor Research, Dublin City University, Glasnevin, Dublin 9, Ireland.

<sup>b</sup>: School of Chemical Sciences, Dublin City University, Glasnevin, Dublin 9, Ireland.

E-mail: [james.walsh@dcu.ie](mailto:james.walsh@dcu.ie)

## Electronic supplementary information

### 1 Experimental

Pyridine, poly(4-vinylpyridine) (4-PVP,  $M_w = 60,000 \text{ g}\cdot\text{mol}^{-1}$ ), methanol (MeOH, 99 %), KCl, NaHCO<sub>3</sub> (> 99 %), Na<sub>2</sub>CO<sub>3</sub>, LiClO<sub>4</sub> (electrochemical grade) were purchased from Sigma Aldrich and used as received. All aqueous solutions were made up using Milli-Q water. The methanolic deposition solution for drop-casting of 4-PVP was 10 mg/200  $\mu\text{L}$  (5 % w/v) and 5  $\mu\text{L}$  drops were cast (*ca.* 250  $\mu\text{g}$  of polymer and thus *ca.* 3.2  $\mu\text{mol}$  of py monomer units). CO<sub>2</sub> (N4.0) was purchased from Air Products.

Cyclic and linear sweep voltammetry was performed using a CHInstruments 660 potentiostat with a gold disc working electrode ( $d = 2 \text{ mm}$ , CHInstruments), a Pt coil counter electrode and a Ag/AgCl (sat. KCl) reference electrode, which was calibrated daily vs. a master saturated calomel electrode. The electrolyte used was either 0.1 M NaHCO<sub>3</sub>/H<sub>2</sub>O or 0.1 M LiClO<sub>4</sub>/MeOH. All solutions were purged with N<sub>2</sub> or CO<sub>2</sub> for 20 minutes prior to experiments and were kept under a blanket of gas throughout. In all cases two CV cycles were recorded and the data shown are from the second cycle. The pH of the solution was 5.3 (N<sub>2</sub> purged) or 3.9 (CO<sub>2</sub> purged).

Electrocatalytic measurements were performed in a custom-made H-cell using a gold disc working electrode either unmodified or coated with a drop-cast film of 4-PVP. The working electrode compartment was sampled periodically for gas products (H<sub>2</sub> and CO) using gas chromatography. Gas chromatography was performed using a Varian CP-3800 employing N5 helium as the carrier gas (20 ml.min<sup>-1</sup>) at 60°C. A 5 Å molecular sieve column (Varian 1041, 3.7 m, 1/8 inch stainless steel) and a pulsed discharge detector (D-3-I-HP, Valco Vici) were employed. CO peak areas were quantified with multiple calibrant gas (200 ppm CO, 200 ppm CH<sub>4</sub>, 500 ppm H<sub>2</sub> in a helium matrix, Calgaz) injections and were re-calibrated daily.

Surface enhanced Raman spectroscopy (SERS) was performed using a Horiba Jobin Yvon HR800 UV spectrometer. The laser (532 nm) was generated by a Coherent Innova 70c solid state Ar-ion laser (532 nm) and a 20x microscope objective. A 600 grooves/mm diffraction grating was employed. The x-axis was calibrated versus the Rayleigh line (0 nm) and the phonon mode from silicon wafer (520 cm<sup>-1</sup>). UV/Vis spectroscopy was performed using a Jasco V750 spectrometer with slit

widths of 1 mm, with films of 4-PVP/MeOH drop-cast onto quartz slides and allowed to dry in air prior to spectral recording. Solution FTIR spectra were recorded using a Perkin-Elmer Spectrum 100 (16 scans, 4 cm<sup>-1</sup> resolution) by placing a drop of solution directly onto a diamond ATR tip. Film thicknesses were measured using a Bruker DektakXT stylus profilometer at a scan speed of 0.1 mm/s.

Surface-enhanced Raman spectroelectrochemistry (SERS SEC) was performed using a CHI Instruments 660 potentiostat as described above. The cell was setup in a glass vial for voltammetry (ALS Japan) and a Teflon cap to hold electrodes in position. The cell was purged with N<sub>2</sub> or CO<sub>2</sub> for 20 minutes prior to experiments and were kept under a blanket of gas throughout. An inverted laser (532 nm) was focussed through the bottom of the glass and onto the working electrode/electrolyte interface. Spectral acquisition was averaged over 4 scans of 8 seconds each.

## 2 pH dependence of films by UV spectral titration and linear sweep voltammetry

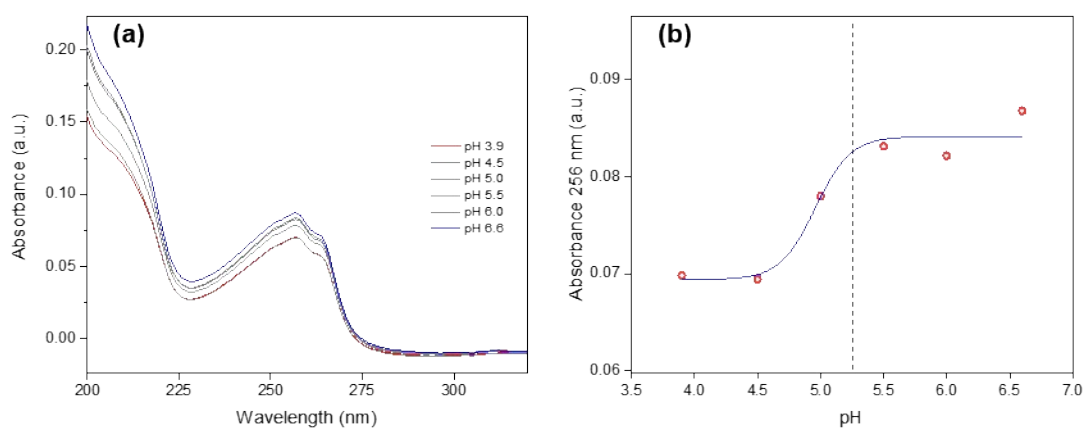


Fig. S1 (a): pH dependence of the UV spectrum of a 4-PVP film drop-cast (5  $\mu$ L of 5 % w/v solution in MeOH) onto a quartz slide. (b) Plot of Abs<sub>256 nm</sub> vs. pH of contact solution is non-linear and shows a pK<sub>a</sub> of ca. 5.0 for 4-PVP, which is similar to the literature value of free pyridine pK<sub>a</sub> dissolved in aqueous solution (dashed line in (b)). The blue line in (b) represents the sigmoidal best fit using a Boltzmann function in Origin 2018 64 bit.

In Fig. S1 (a) the changes in absorbance of the  $\pi$ - $\pi^*$  transition centred at 256 nm are most likely due to the differences in UV absorption of the pyridine and pyridinium forms of the species.<sup>S1</sup> The transformation from one form to the other is not quantitative, based on reported molar extinction coefficients for py and pyH<sup>+</sup> monomers,<sup>S1</sup> suggesting that not all py units are protonated to pyH<sup>+</sup>. An isosbestic point was not observed, potentially due to physical changes occurring throughout the film; indeed, swelling and contraction of 4-PVP films in contact with solution of pH above and below the pK<sub>a</sub> of py has been shown previously.<sup>S2</sup> Additionally, the py and pyH<sup>+</sup> spectra exhibit  $\lambda_{\text{max}}$  values that differ by a reported 0.5 nm only,<sup>S1</sup> suggesting overlap of the two spectra at a given wavelength is unlikely. Attempts to conduct equivalent studies into the protonation state of the film as a function of contact solution pH using <sup>15</sup>N-NMR spectroscopy were unsuccessful.<sup>S3</sup> In this experiment, a film of 4-PVP was deposited from MeOH on the inner walls of a standard NMR tube and allowed to dry overnight in air. The NMR solvent used was D<sub>2</sub>O pD-corrected<sup>S4</sup> using NaOD or DCl to pD values of ca. 8 and 3 respectively; however, only spectra of the blank electrolyte in an unmodified tube could be

acquired with the spectrometer unable to lock on the PVP-coated tube. Future experiments will focus on the development of a manual locking protocol to monitor these spectral changes.

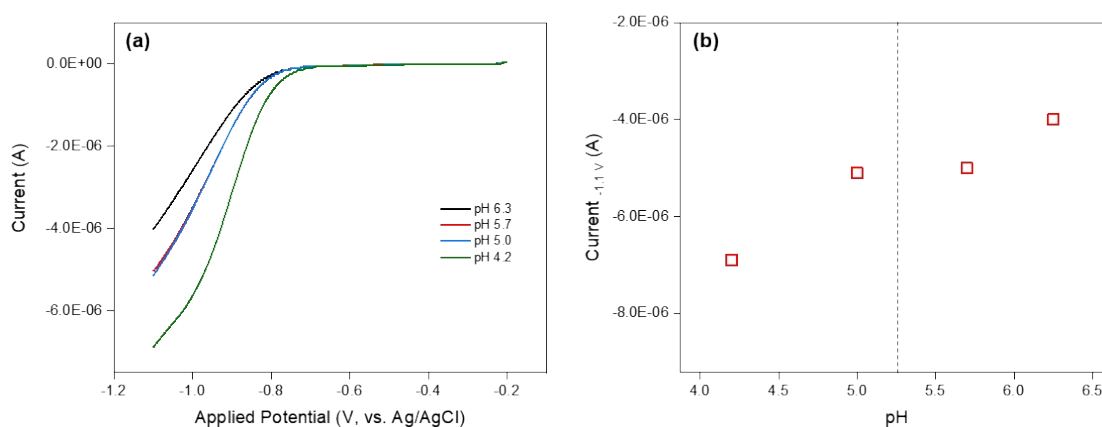


Fig. S2: pH dependence of CVs of a 4-PVP film drop-cast (5  $\mu\text{L}$  of 5 % w/v solution in MeOH) on Au WE under CO<sub>2</sub> in 0.5 M KCl. Current max at -1.1 V vs. Ag/AgCl shows pH dependence is non-linear around the literature pK<sub>a</sub> value of pyridine dissolved in aqueous solution (dashed line in (b)).

### 3 Film thickness by profilometry

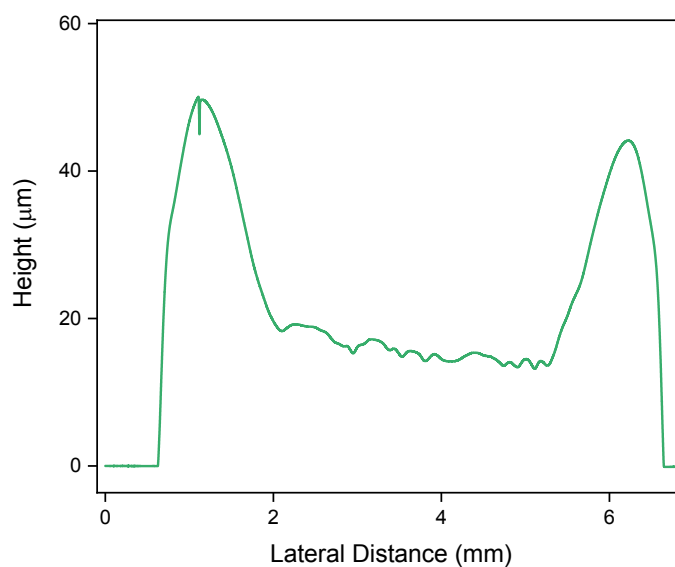


Fig. S3: Profilometry of a 4-PVP film drop-cast (5  $\mu\text{L}$  of 5 % w/v solution in MeOH) onto Au foil.

### 4 Controlled potential electrolysis

Electrode	V, vs. Ag/AgCl	V, vs. RHE	FE H <sub>2</sub>	FE CO	FE Total
Au	-0.9	-0.376	71	0	71
Au/4-PVP	-0.9	-0.376	75	0	75
Au	-1.2	25	64	89	
Au/4-PVP	-1.2	-0.676	11	68	79

Table S1: CPE data for Au foil electrode (area = 0.7 cm<sup>2</sup> approx.) for unmodified and 4-PVP film-modified electrodes. Electrolysis was conducted in a CO<sub>2</sub>-purged H-cell for 30 minutes. No formate was detected in the catholyte post-experiment by <sup>1</sup>H-NMR.

## 5 Raman and FTIR spectroscopy

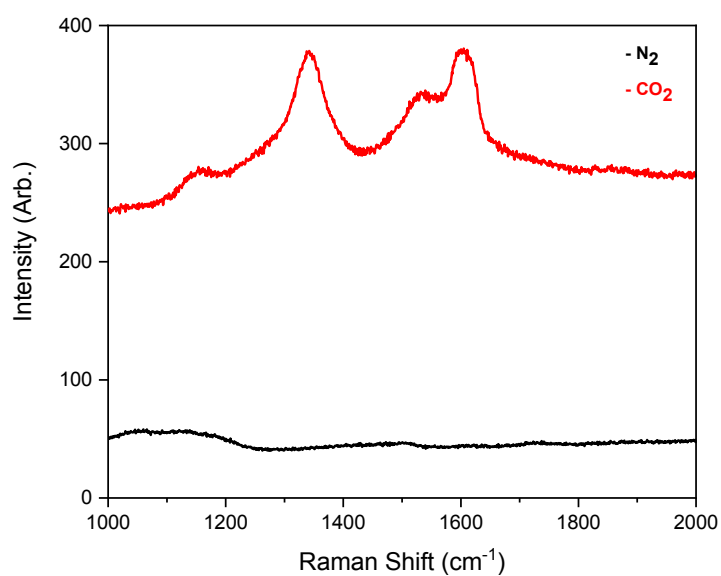


Fig. S4: SERS of a blank, unmodified Au electrode in N<sub>2</sub>-purged 0.5 M KCl under a blanket of N<sub>2</sub> (black). After CO<sub>2</sub> purging of the same solution, four intense Raman modes appear (red).

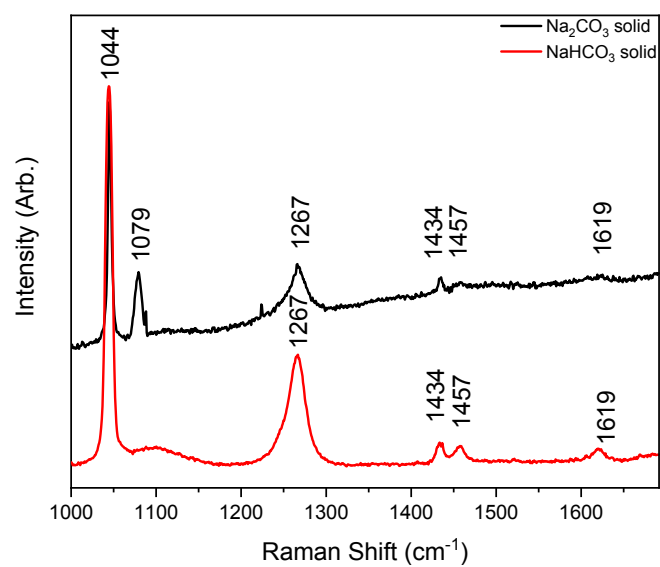


Fig. S5: Raman spectra of solid  $\text{NaHCO}_3$  and  $\text{Na}_2\text{CO}_3$  crystals.

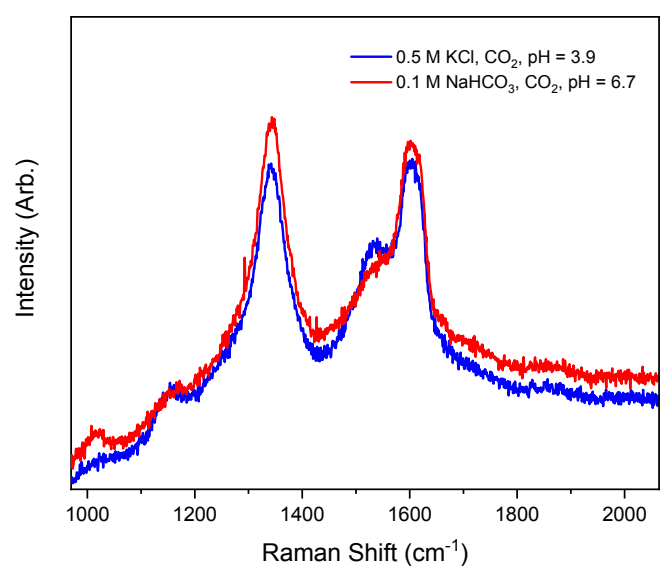


Fig. S6: SERS of Au disc electrode in different electrolytes and at different pH values.

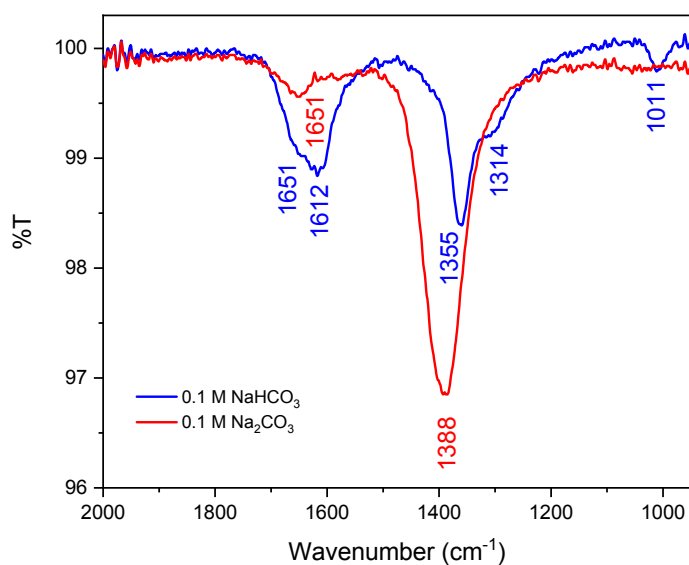


Fig. S7: ATR-FTIR spectra of 0.1 M solutions of NaHCO<sub>3</sub> and Na<sub>2</sub>CO<sub>3</sub>.

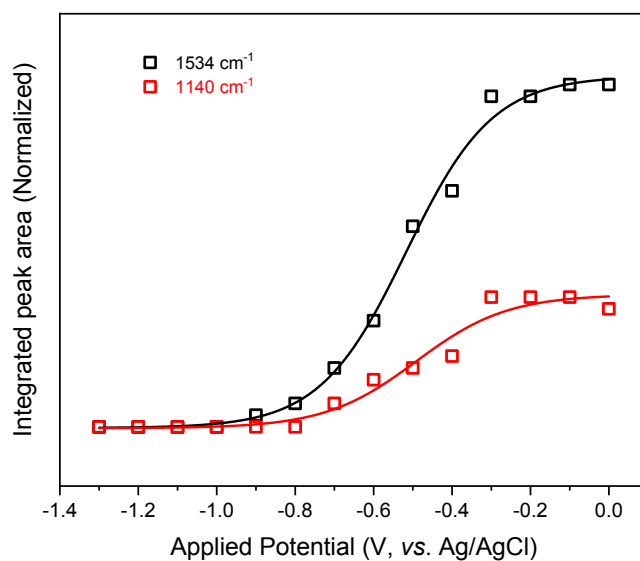


Fig. S8: Integrated areas from peak-fitted SERS spectra of a blank, unmodified Au electrode in CO<sub>2</sub>-purged 0.5 M KCl/H<sub>2</sub>O electrolyte at all applied potentials showing loss of modes at 1534 and 1140 cm<sup>-1</sup> occurs simultaneously and are therefore attributed to the same species (adsorbed deprotonated HCO<sub>3</sub><sup>-</sup> as CO<sub>3</sub><sup>2-</sup>). The solid lines represent sigmoidal best fits using a Boltzmann function in Origin 2018 64 bit.

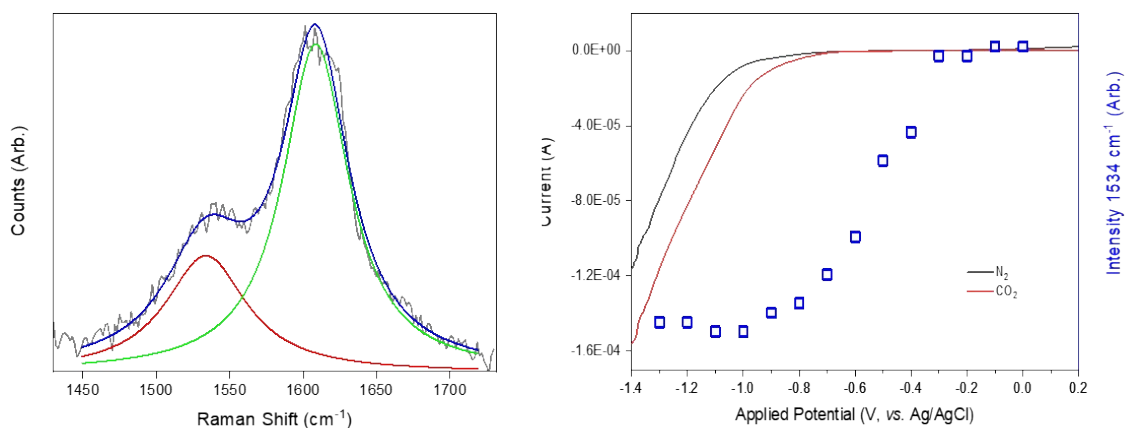


Fig. S9 (a): Peak-fitted SERS of a blank, unmodified Au electrode in  $\text{CO}_2$ -purged 0.5 M KCl/ $\text{H}_2\text{O}$  electrolyte at -0.5 V a broad band at  $1608\text{ cm}^{-1}$  and a shoulder at  $1534\text{ cm}^{-1}$ . The band at  $1608\text{ cm}^{-1}$  can itself be peak fit to show two maxima at  $1598$  and  $1620\text{ cm}^{-1}$ , potentially corresponding to the OH bend of interfacial water<sup>S5</sup> in addition to the  $\nu_{\text{as}}$  C-O stretch of chemisorbed deprotonated bicarbonate, but in Fig. S9 (a) the fit has been reduced to two peaks for simplicity. Grey: raw recorded data; green and red: fits to the two maxima; blue: summation of red and green curves. (b) Linear sweep voltammetry of a blank Au electrode in 0.5 M KCl/ $\text{H}_2\text{O}$  electrolyte under  $\text{N}_2$  (blank) and  $\text{CO}_2$  (red) atmospheres. The blue squares show that the disappearance of the adsorbed bicarbonate mode at  $1534\text{ cm}^{-1}$  does not correlate with electrocatalytic potentials for HER or  $\text{CO}_2\text{RR}$ . The data were fit to a series of overlapping Lorentzian peaks using the function  $y = y_0 + (2 \cdot A / \pi) \cdot (w / (4 \cdot (x - xc)^2 + w^2))$  in Origin 2018 64 bit.

An excellent fit of the spectrum shown in Fig. S9(a) revealed two modes with maxima at  $1540$  and  $1610\text{ cm}^{-1}$  (broad). There may be some asymmetry in the mode at  $1610\text{ cm}^{-1}$  and a reasonable fit could be attained with three maxima at  $1540$ ,  $1598$  and  $1620\text{ cm}^{-1}$ . This could correspond to the two modes of physisorbed and chemisorbed bicarbonate, as well as the interfacial bending mode of adsorbed  $\text{H}_2\text{O}$  at  $1620\text{ cm}^{-1}$ , consistent with previous studies.<sup>S5</sup> This fit was not as high quality as that shown in Fig. S9(a), however, so the discussion herein is presented in terms of the broad mode at  $1610\text{ cm}^{-1}$ . This feature may be more clearly resolved at higher resolution in future studies.

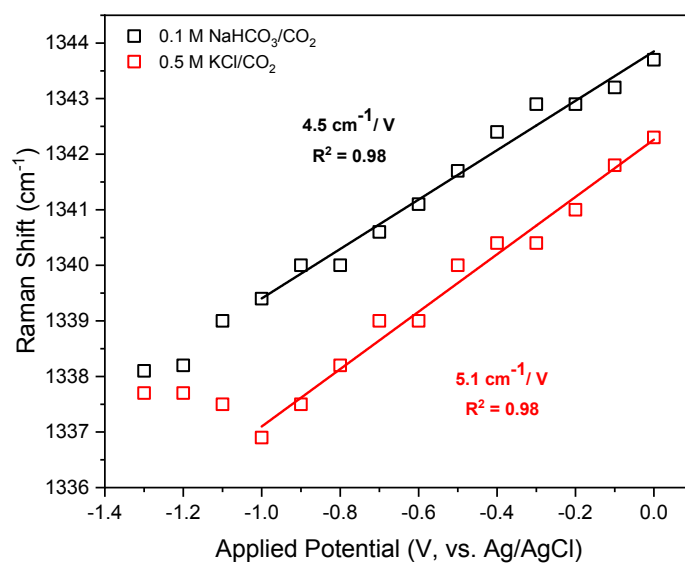


Fig. S10: Plot of peak maxima at *ca.* 1340 cm<sup>-1</sup> ( $\nu_s$  C-O stretch of chemisorbed deprotonated bicarbonate) for unmodified Au disc electrodes in the presence of different electrolytes. The Stark shifts of approximately 5 cm<sup>-1</sup>.V<sup>-1</sup> for both systems are indicative of chemisorption and the lack of Stark shifting for the modes at 1140 and 1534 cm<sup>-1</sup> implies that these modes are due to non-chemisorbed (i.e.: physisorbed) species.

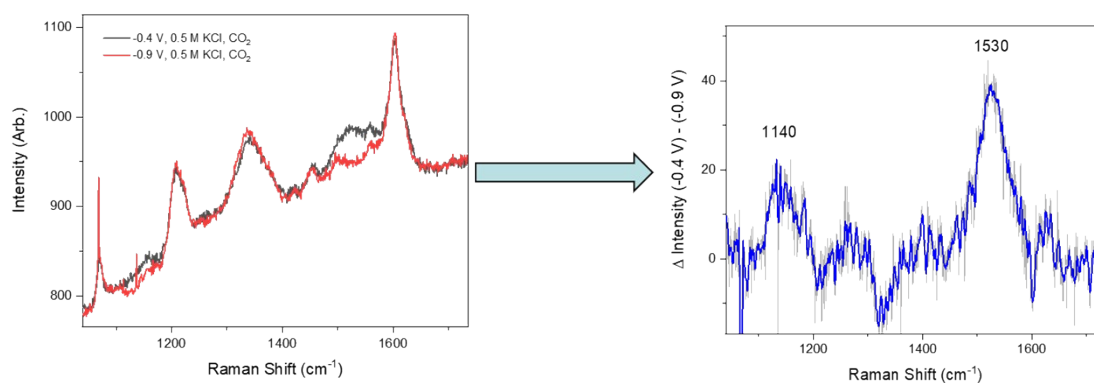


Fig. S11: A difference spectrum shows the changes in intensity between spectra acquired at -0.4 V and -0.9 V for a PVP-coated Au disc WE in CO<sub>2</sub>-purged 0.5 M KCl. The greatest changes in intensity are at approximately 1530 and 1140 cm<sup>-1</sup>, which correlates with the spectral changes in Figs. 3, S8 and S9 and are attributed to the desorption of physisorbed deprotonated bicarbonate through cracks in the thick PVP film. No spectral signal was observed for the chemisorbed bicarbonate, indicative of surface blocking by the PVP layer. Smoothing (blue) was performed using the Savitsky-Golay function with a 2<sup>nd</sup> order polynomial and a ten data point window.



## References

- S1 T. Handa, Y. Utena, H. Yajima, T. Ishii and H. Morita, *J. Phys. Chem.*, 1986, **90**, 2589–2596.
- S2 Y. Wang, V. Kozlovskaya, I. G. Arcibal, D. M. Cropek and E. Kharlampieva, *Soft Matter*, 2013, **9**, 9420–9429.
- S3 W. Jiang, L. Lumata, W. Chen, S. Zhang, Z. Kovacs, A. D. Sherry and C. Khemtong, *Sci. Rep.*, 2015, **5**, 1–6.
- S4 A. Krezel and W. Bal, *J. Inorg. Biochem.*, 2004, **98**, 161–166.
- S5 D. Bohra, I. Ledezma-Yanez, G. Li, W. De Jong, E. A. Pidko and W. A. Smith, *Angew. Chem. Int. Ed.*, 2019, **58**, 1345–1349.